Influence of surface properties on the dynamics of fluid flow

E. Istenič, V. Šajn and M. Brojan

View Online

Export Citation
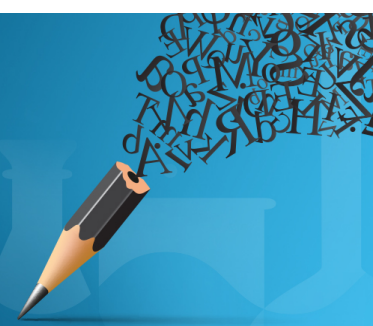
CrossMark

Influence of surface properties on the dynamics of fluid flow

View Online   Export Citation   CrossMark

E. Istenič, V. Šajn, and M. Brojan[a] (iD)

AFFILIATIONS

Laboratory for Nonlinear Mechanics, Faculty of Mechanical Engineering, University of Ljubljana, Aškerčeva 6, SI-1000 Ljubljana, Slovenia

[a]Author to whom correspondence should be addressed: miha.brojan@fs.uni-lj.si

ABSTRACT

In this paper, we study how the fluid flow near the surface of a monocrystalline body is affected by the surface properties due to atom-surface scattering. We propose a toy model for this system by parameterizing the surface with a periodic function of the tangential position. This allows us to derive the velocity probability density function in the Knudsen layer and determine statistical averages of fluid velocity and stress tensor components in the region of interest. The results of this analysis provide a potentially more fundamental and accurate explanation for empirically observed phenomena such as the no-slip boundary condition, boundary layer formation, and the onset of hydrodynamic instability.

I. INTRODUCTION

We consider the problem of fluid flow in a semi-infinite domain bounded by the surface of a solid body (wall) and assume that the surface moves with a constant velocity along a stationary body of fluid. The setup is shown by Fig. 1.

This setup represents a simple model of fluid motion induced by a translating body adjacent to the fluid, where we call this mode of fluid motion a boundary layer. Understanding the formation and evolution of boundary layers depending on various external parameters is of great importance in different branches of physics and engineering. For example, boundary layers determine hydrodynamic and aerodynamic characteristics of ships and aircraft, they influence convective heat transfer in steam and gas turbines, which determines their operational temperature ranges, they are the cause behind the Magnus effect experienced by rotating bodies moving through fluids, and they appear in various other fields, such as microfluidics, sediment transport, and meteorology.

The problem of boundary layer formation and evolution is usually considered to have been well understood for some time, as solutions of, for example, Navier–Stokes equations describing the boundary layer velocity field have been known for some time. Furthermore, the linear relationship between fluid velocity and shear stress is a well-known fact. However, theoretical deliberations explaining this phenomenon have made an assumption (simplification) that

the surface along which a boundary layer is generated is ideally flat with no geometric perturbations on any length scale. While the surface of a solid body may appear flat on the macroscopic length scale, it is in fact corrugated on the atomic length scale ($\sim 10^{-10}$ m). We reason that this corrugation affects fluid velocity and stress tensor components, that is, boundary conditions that appear in the theoretical problems previously mentioned, and that it is the cause of tangential stress present at the fluid-solid boundary as well as perturbations, which lead to flow instability and the onset of turbulence. Our intent to understand fluid behavior in the vicinity of the surface is therefore also motivated by practical applications, such as development of wall functions utilized in computational fluid dynamics, which would account for surface characteristics and allow for more physically accurate and realistic calculations. Understanding the dependence of boundary layer formation, evolution, and its stability on the characteristics of the surface boundary would therefore enable us to design superior turbomachinery, ships, and aircraft and allow us to gain a more complete understanding of various natural phenomena.

The flow of fluid past rough surfaces or surfaces with spatially variable geometry is an active field of research, as can be seen from the comprehensive review by Kadivar et al.[1] Several papers have been written which analyze the problem through the formalism of continuum mechanics and numerical simulations, such as those by Dharaiya and Kandlikar,[2] as well as by Rouhi et al.[3] Theoretical analysis of the
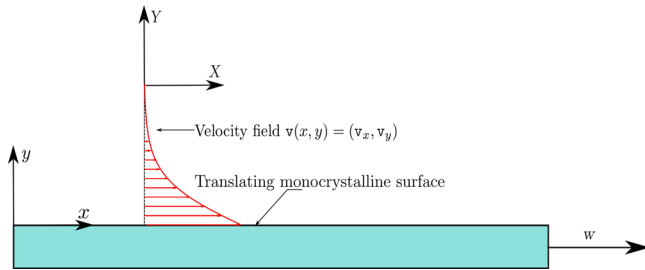
FIG. 1. Fluid flow induced by a moving surface.

influence of atom-surface scattering on the dynamics of fluid flow near surfaces is also a field of research, which has seen plenty of progress. Comprehensive reviews of the subject are provided by Cercignani,[4] Sharipov and Seleznev,[5] and Roldughin and Zhdanov,[6] while Golse and Takata analyzed properties of the Boltzmann equation, which are important when analyzing bounded flows and boundary layers in Refs. 7 and 8. A number of papers pertaining to the analysis of shear flows in different settings by means of the kinetic theory of gases, and determine solutions to the Boltzmann equation and slip coefficients while assuming various scattering models at fluid solid boundaries, for example, by Cercignani,[9,10] Loyalka,[11,12] Kuščer and Klinc,[13] Siewert and Garcia,[14–16] Wu and Struchtrup,[17] Nguyen and Graur,[18] and Chen[19] have been written, while several authors tackled similar problems using both a combination of kinetic theory formalism and molecular dynamics simulations, such as Wang et al.[20,21] Several papers have also been written which determine slip coefficients at fluid solid boundaries using the Kubo–Greenwood formalism, such as those by Nakano and Sasa,[22] and De la Torre and Duque-Zumajo.[23]

Other authors used solutions of the Boltzmann equation for physically similar cases to obtain expressions for velocity fields, for example, by Gross, Jackson, and Ziering[24–26] and Aoki.[27] Various other papers present how gas-surface scattering models form the basis for determining boundary conditions used to solve either the Boltzmann equation (kinetic theory) or Navier–Stokes equations (continuum-based approach), such as papers authored by Brull,[28] Coron,[29] Shen, Chen et al.,[30] Hattori et al.,[31] Aoki et al.,[32] Kosuge et al.,[33] and Duan.[34] Other papers analyzed flow of gases near solid surfaces using both analytical and numerical methods (lattice Boltzmann method or molecular dynamics) in the scope of kinetic theory, such as Ben-Ami and Manela,[35] while other authors considered numerical approaches only, such as Silva et al.,[36,37] Mohammed and Reis,[38] Shan,[39] Ou and Chen,[40] Liang et al.,[41] and Varghese et al.[42] Most of these previously mentioned deliberations assumed simple atom-surface scattering models, such as the diffuse-specular scattering kernel, which does not account for any spatial variations of scattering properties, and focused on solving the Boltzmann equation and determining statistical averages in an entire domain of fluid adjacent to the surface in question.

In the present study, we determine expressions for velocity and stress tensor components in the Knudsen layer, that is, at the solid–fluid boundary, while accounting for spatial variations of scattering properties caused by the surface corrugation. We achieve this by describing these variables as statistical averages of corresponding microscopic variables, wherein we average them over probability density functions (PDFs), which depend on the position along the surface and its properties. We assume that the fluid behaves as an ideal gas, which means that there are no long-range intermolecular forces and that there is no adsorption of molecules on the surface. We also assume that surface corrugation occurs only in the x–y plane despite the fact that crystals are three-dimensional objects and that scattering along the z axis does not have a significant influence on the behavior of fluid in the Knudsen layer as there is no (macroscopic) relative motion in the direction of z axis. This renders our analysis considerably easier.

We will solve the problem presented by determining the probability density function of particle velocities in the Knudsen layer and using this function to obtain statistical averages of the fluid velocity components as well as the stress tensor components. We will determine the previously mentioned probability density function by first defining a conditional probability density function P, which determines the probability of a particle scattering off the surface with a certain velocity given some other velocity of incidence and can be expanded as a trigonometric series of the tangential coordinate x. Second, we will integrate the product of the velocity probability function pertaining to incident particles f^-, which we assume to be a Maxwell–Boltzmann distribution function, and the condition probability density function P in order to obtain the velocity probability density function of particles, which have scattered of the surface f^+. We then combine f^- and f^+ to form a complete velocity probability function f and use to obtain the previously mentioned statistical averages.

Because of Galilean relativity of velocities, this setup is equivalent to the flow of a fluid along the surface of a stationary solid body. This model of a physical system can be parameterized in Cartesian coordinates in the following way:

$$X \in (-\infty, \infty),$$
$$Y \in [Y_S, \infty), \qquad (1)$$
$$Z \in (-\infty, \infty).$$

We also introduce a reference system which moves in unison with the surface, according to which we parameterize the model as

$$x \in [0, \infty),$$
$$y \in [y_S, \infty), \qquad (2)$$
$$z \in (-\infty, \infty).$$

Surface corrugation is a consequence of the way potentials determining intermolecular interactions combine when the atoms, which constitute a solid body, are arranged in a crystal lattice. If we choose to describe the physical system under consideration with Cartesian coordinates, we can parameterize the potential as

$$U(x, y, z) = \begin{cases} \infty, & y \leq f_S(x), \\ 0, & y > f_S(x), \end{cases} \qquad (3)$$

where the function $f_S(x)$ is equal to

$$f_S(x) = \frac{h_0}{2} \cos \frac{2\pi x}{L_0}, \qquad (4)$$

with h_0 and L_0 representing the peak-to-peak amplitude and wavelength/wave period, respectively. Function f_S defining the shape of the

potential at the atomic length scale, where corrugation is apparent, therefore represents the lower bound of fluid domain y_S from Eq. (2). This means that $y_S = f_S(x)$. However, as we make the transition in our description from the atomic to the macroscopic length scale, we can simplify this by stating that $y_S \approx 0$, which means that the domain boundaries are (approximately) equal to

$$
\begin{aligned}
x &\in [0, \infty), \\
y &\in [0, \infty), \\
z &\in (-\infty, \infty).
\end{aligned}
\tag{5}
$$

The physical system under consideration is displayed in Fig. 2.

Boundary values of velocity and stress tensor components are in the classical continuum mechanics-based analysis assumed to hold true in the direct vicinity of the surface, that is, for $y = 0$. Since the macroscopic quantities are statistical averages of the microscopic equivalents, boundary values near the surface are in fact valid in the region

$$
\begin{aligned}
x &\in [0, \infty), \\
y &\in [y_S, L_{\text{Kn}}), \\
z &\in (-\infty, \infty),
\end{aligned}
\tag{6}
$$

where L_{Kn} is the thickness of the Knudsen layer. This is a part of the fluid domain closest to the wall where gas atom–surface interactions dominate interactions between individual gas molecules, as the likelihood of gas molecule collision with the surface is significantly greater than the likelihood of collisions between individual gas molecules. The upper vertical boundary of the Knudsen layer can be defined as the average vertical distance a molecule travels before colliding with another molecule. Therefore, it is reasonable to assume that incident and scattered molecules do not collide or otherwise interact while traveling through the Knudsen layer.

The thickness of the Knudsen layer is usually of the same order of magnitude as the molecular mean free path l_{mfp},

$$
L_{\text{Kn}} = \frac{2}{3} l_{\text{mfp}} = \frac{\sqrt{2}}{3\pi} \frac{k_B T}{p d^2},
\tag{7}
$$

where k_B, T, p, and d are the Boltzmann constant ($k_B = 1.380\,648\,81 \times 10^{-23}$ J/K), temperature, static pressure, and particle kinetic
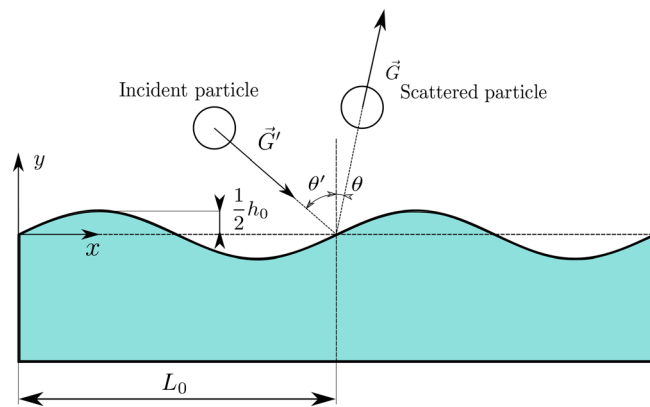

FIG. 2. Particle scattering on a monocrystalline surface.

diameter, respectively. The factor of $\frac{2}{3}$ is present because it is equal to the average height of a unit hemisphere, as particles will on average travel a distance of $\frac{2}{3} l_{\text{mfp}}$ in the direction perpendicular to the surface. Because the Knudsen layer thickness is of the order of the molecular mean free path, it is miniscule compared to the characteristic dimensions of the flow (when dealing with macroscopic fluid flows) at normal atmospheric conditions, but at the same time, it is several orders of magnitude greater than the corrugation amplitude. This is why we can neglect its physical size and claim that the values quantities have in the Knudsen layer are equal to the values for $y = 0$, which defines the fluid-solid contact line as given by Eq. (5). Vertical position of the upper bound of the Knudsen layer in the global reference frame, Eq. (1), shall henceforth be denoted as y_{Kn}.

Macroscopic quantities, such as density, velocity, and stress tensor components as well as internal energy, can be derived by statistically averaging their microscopic equivalents. This operation calls for a probability density function (PDF) f, $f(r_i, v_i, t)$, $i \in \{x, y, z\}$, which determines the probability density of the N particles present in the physical system being at certain positions in space and having particular velocities. Statistical average of a property pertaining to individual particles, which is a function of position r_i and particle velocity v_i, is equal to the expression determined by the following integral:

$$
\begin{aligned}
\Psi(r_i, t) &= \langle \psi(r_i, v_i) \rangle \\
&= \iiint_{\partial \text{P.S.}} \psi(r_i, v_i) f(r_i, v_i, t) \, dv_i \, dv_j \, dv_k,
\end{aligned}
\tag{8}
$$

where ∂P.S. denotes all of the microstates in velocity phase space which a particular system can occupy under specific conditions. Furthermore, we can also take statistical averages over spatial coordinates as shown here

$$
\begin{aligned}
\Psi(t) &= \langle \psi(r_i, v_i) \rangle \\
&= \oint_{\partial V} \iiint_{\partial \text{P.S.}} \psi(r_i, v_i) f(r_i, v_i, t) \, dv_i \, dv_j \, dv_k \, dr_i \, dr_j \, dr_k,
\end{aligned}
\tag{9}
$$

where we average over a spatial volume (a volume in coordinate space) denoted by ∂V. We should note the important fact that statistical averages of microscopic variables correspond to variables relevant in continuum mechanics as long as the PDF is not spatially dependent on length scales smaller than the minimum length scale L_{min} at which the assumption of continuum holds true. Because statistical averaging only makes sense when an ensemble enclosed by some volume contains a sufficient number of particles, the assumption of continuum breaks down at some point with decreasing length scales determining the volume, at which point statistical averages do not correspond to macroscopic, that is, continuum variables, but rather some sort of mesoscopic variables (assumption of continuous matter makes it seem as if we can determine values of particular variables for an infinite number of points in space, when in fact we can do so only for a finite number of points, which determine the positions of volume elements that are sufficiently large for statistical averages to correspond to macroscopic values). This means that any spatial variations of the PDF at length scales smaller than L_{min} will express themselves in the form of intermediate mesoscopic quantities. Their spatial averages can still represent quantities relevant to the continuum based description, but spatial averaging may also filter out any variations present below L_{min}.

The probability density function corresponding to a particular physical system is governed by the Boltzmann equation

$$\frac{\partial f}{\partial t} + v_i \frac{\partial f}{\partial r_i} + \frac{F_i}{m_p} \frac{\partial f}{\partial v_i} = Q(f, f). \tag{10}$$

Here, F_i represents the external force and $Q(f,f)$ is the collision integral operator and is, in general, determined by the expression

$$Q(f,f) = \int\int\int (f'_1 f' - f_1 f)\, g_i(v_i, v_{1,i})\, R(\Omega, g)\, d\Omega\, dv_{1,i}, \tag{11}$$

where $g_i(v_i, v_{1,i})$ is the absolute value of relative collisional velocities, and $R(\Omega, g)$ is the collision cross section, which is generally a function of the relative velocity g and solid angle Ω. Functions $f_1, f, f'_1,$ and f' are probability density functions pertaining to a pair of colliding particles determining the probabilities of pre- and post-collisional velocities. Throughout the text, primed and non-primed variables denote quantities before and after collisions, either in the context of collisions of particles in the bulk or collisions of particles with the solid surface.

When colliding particles have equal masses, their post-collisional velocities are determined as

$$\begin{aligned} v_{1,i} &= v'_{1,i} - (g_j k_j) k_i, \\ v_i &= v'_i - (g_j k_j) k_i, \end{aligned} \tag{12}$$

where k_i stands for the unit vector element pointing from the mass center of one colliding particle to another. These relations can be derived from the equations describing conservation of momentum

$$m_p v'_i + m_p v'_{1,i} = m_p v_i + m_p v_{1,i}, \tag{13}$$

and energy

$$\frac{1}{2} m_p v'_i v'_i + \frac{1}{2} m_p v'_{1,i} v'_{1,i} = \frac{1}{2} m_p v_i v_i + \frac{1}{2} m_p v_{1,i} v_{1,i}. \tag{14}$$

It is also worth mentioning that the validity of the Boltzmann equation at different length and time scales is still a subject of intense discussion, with a number of papers written regarding this issue, including works by Lanford,[43] Illner and Pulvirenti,[44] Kuzovlev,[45] Esposito et al.,[46] and Gallagher.[47] Kuzolev states that in cases when one can expect the molecular velocity probability density function to be spatially inhomogeneous on length scales close to or smaller than the molecular mean free path due to spatially inhomogeneous external forces or kinematic considerations, as in our case, the validity of Boltzmann equation, as given by Eq. (10), is debatable, or the expression for the collision operator given by Eq. (11) takes on a different form. This issue becomes less contentious if the assumptions of the model allow us to neglect the collision operator.

In general, solutions to the Boltzmann equation are eigenfunctions of the collision operator $Q(f,f)$ as given by Eq. (11), or some linear combination of them. The simplest possible solution for a system in thermodynamic equilibrium is the Maxwell–Boltzmann distribution/ probability density function

$$f_0 = n \left(\frac{m_p}{2\pi k_B T}\right)^{\frac{3}{2}} e^{-\frac{m_p (v_i - v_i)^2}{2 k_B T}}, \tag{15}$$

where n is the number density (number of particles per unit of volume). Another solution, which describes cases when the system is slightly out of equilibrium, is

$$f = f_0 \left(1 - \frac{A}{T} c_i \frac{\partial T}{\partial r_i} - \frac{m_p B}{k_B T} c_i c_j \frac{\partial v_i}{\partial r_j}\right), \tag{16}$$

where we introduced relative velocity $c_i = v_i - v_i$, with v_i being the statistical average of a velocity component as determined by Eq. (8). Functions A and B are functions of density, temperature, and the absolute value of relative velocity: $A(\rho, c^2, T), B(\rho, c^2, T)$, and are determined by the eigenvalues of the Boltzmann integral collision operator.

In the region close to the wall whose bounds are defined by expression Eq. (6), we assumed that no collisions between individual particles take place. This means that we can deal with a simplified Boltzmann equation which lacks the integral collision operator, the solutions of which are independent of non-equilibrium contributions. Therefore, we assume that velocity probabilities in the Knudsen layer region are determined by a function proportional to Eq. (15). We can write the velocity PDF of particles as a sum of contributions determining probabilities pertaining to incident and scattered particles, as shown here

$$f = \frac{1}{2}(1 - \text{sgn}(v_y)) f^-(v_i) + \frac{1}{2}(1 + \text{sgn}(v_y)) f^+(v_i), \tag{17}$$

where $f^-(v_i)$ and $f^+(v_i)$ are the PDFs pertaining to the incident ($v_y < 0$) and scattered particles ($v_y > 0$) as shown in Fig. 3. Because we assumed that incident and scattered particles do not interact while traveling through the Knudsen layer, we can simply split Eq. (17) into two parts, where f^+ is obtained by some transformation of f^- which is a consequence of scattering.

Before we discuss these functions further, we introduce transformations of the velocity coordinates which enables us to simplify the description. These transformations are shown in Fig. 4. First, we transform particle velocities from being relative to the global reference frame as shown in Fig. 1 to being relative to the reference frame which moves in unison with the translating surface

$$\begin{aligned} u'_x &= v'_x - w, \\ u'_y &= v'_y, \\ u'_z &= v'_z, \\ u_x &= v_x - w, \\ u_y &= v_y, \\ u_z &= v_z, \end{aligned} \tag{18}$$

where u_x, u_y, and u_z are velocities in the local reference frame, Eq. (2). Second, we transform velocity coordinates into cylindrical form
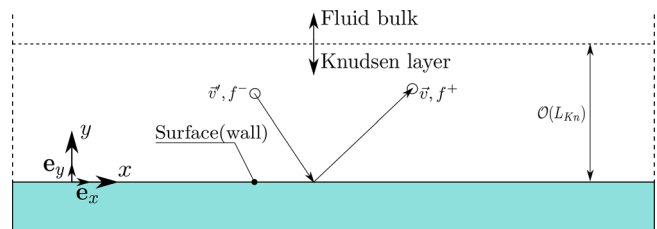

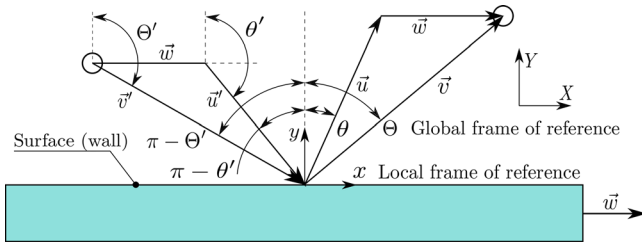FIG. 3. Knudsen layer (particles and the wall are not drawn to scale).

FIG. 4. Kinematic quantities that appear in Eqs. (18)–(20).

$$
\begin{aligned}
u'_x &= u'_0 \sin \theta', \\
u'_y &= u'_0 \cos \theta', \\
u'_z &= u'_z, \\
u_x &= u_0 \sin \theta, \\
u_y &= u_0 \cos \theta, \\
u_z &= u_z.
\end{aligned} \tag{19}
$$

Velocity components relative to the global frame of reference are therefore equal to

$$
\begin{aligned}
v'_x &= u'_0 \sin \theta' + w, \\
v'_y &= u'_0 \cos \theta', \\
v'_z &= u'_z, \\
v_x &= u_0 \sin \theta + w, \\
v_y &= u_0 \cos \theta, \\
v_z &= u_z.
\end{aligned} \tag{20}
$$

These transformations enable us to describe the PDFs in terms of the absolute value of planar velocity $u_0 = \sqrt{u_x^2 + u_y^2}$, which we assume to be a quantity conserved during interactions with the surface as we assume collisions to be elastic (the same holds true for the equivalent quantity pertaining to velocities in the global reference frame $v_0 = \sqrt{v_x^2 + v_y^2}$).

The determinant of the Jacobian matrix of the two combined transformations is equal to

$$
J(u_i) = \det(\mathbf{J}(\mathbf{u_i})) = \begin{vmatrix} \dfrac{\partial v_x}{\partial u_0} & \dfrac{\partial v_x}{\partial \theta} & \dfrac{\partial v_x}{\partial u_z} \\[6pt] \dfrac{\partial v_y}{\partial u_0} & \dfrac{\partial v_y}{\partial \theta} & \dfrac{\partial v_y}{\partial u_z} \\[6pt] \dfrac{\partial v_z}{\partial u_0} & \dfrac{\partial v_z}{\partial \theta} & \dfrac{\partial v_z}{\partial u_z} \end{vmatrix} = -u_0. \tag{21}
$$

II. ANGULAR PROBABILITY DENSITY OF SCATTERING

This part of the paper addresses the function $P_\theta(\theta', \theta, x)$, which is used to obtain an expression for Eq. (17). This function determines the conditional probability density of particles scattering off the surface at an angle θ relative to the y axis under the condition of particles being incident at an angle θ', and will from this point forth be referred to as the angular probability density of scattering. Figure 2 provides a graphical description of the physical system, where the potential field shown in the image is defined by the previously mentioned Eq. (4).

An expression for the aforementioned function has been obtained by methods, which follow from the formalism of quantum mechanics. Its derivation presumes elastic scattering of atoms from crystal surfaces and therefore relies on the hard corrugated surface model. Basic formalism, which represents the basis for theoretical analysis of gas-surface scattering, is explained in considerable detail by Goodman.[48] The aforementioned expression is a result of work by Ford and Wheeler,[49] Masel *et al.*,[50] Manson,[51] Goodman,[52] and Garibaldi *et al.*[53] Further theoretical deliberations concerning this problem are presented in papers authored by Farias and Rieder,[54] Gumhalter,[55] Guantes *et al.*,[56] and Manson.[57] According to these references, angular probability density of scattering $P_\theta(\theta, \theta')$ along the x axis can be written as a Fourier series of the form

$$
P_\theta(\theta, \theta', r_j) = \sum_{m \in \mathbb{Z}} P_G(\theta, \theta') \, e^{i\frac{2\pi m x}{L_0}}, \tag{22}
$$

where x is the tangential coordinate, i denotes the imaginary unit, and m belongs to the set of integers. Coefficients $P_G(\theta, \theta')$ are in accordance with the previously mentioned references equal to

$$
P_G(\theta, \theta') = \frac{\cos \theta}{\cos \theta'} \, |A_G|^2. \tag{23}
$$

If scattering occurs along the x axis, using certain approximations coefficients displayed above can be written as

$$
P_G(\theta, \theta') = \frac{\cos \theta}{\cos \theta'} J_0^2(c) \, J_{|m|}^2(c), \tag{24}
$$

where $J_m(x)$ is the m-th order Bessel function of the first kind, while the variable c is equal to

$$
c = \frac{1}{2} h_0 k \left(\cos \theta' + \cos \theta \right), \tag{25}
$$

where k is the wave vector corresponding to the particle De Broglie wavelength λ_{DB}. It accounts for the wave-like behavior of massive (in the sense of possessing mass) particles impinging on the surface and is related to their mass and velocity (i.e., momentum) as follows:

$$
\lambda_{\mathrm{DB}} = \frac{h}{m_{\mathrm{p}} v_0}, \tag{26}
$$

where h is the Planck's constant ($h = 6.626\,070\,15 \times 10^{-34}$ J s), while m_{p} and v_0 are the particle mass and the magnitude of its velocity relative to the inertial frame of reference in which the surface is static. The corresponding wave vector is consequently equal to

$$
k = \frac{2\pi}{\lambda_{\mathrm{DB}}} = 2\pi \frac{m_{\mathrm{p}} v_0}{h}. \tag{27}
$$

Because the product of the particles' wave vector k and the peak-to-peak amplitude h_0 is typically a very small number, we can make use of the following approximation, which holds true for small values of c ($c \ll 1$):

$$
J_{|m|}^2(c) \approx \frac{\left(\frac{1}{2} c \right)^{2|m|}}{(|m|!)^2}, \tag{28}
$$

which therefore allows us to simplify the expression Eq. (23) to the following form:

$$P_G(\theta, \theta') = \frac{\left(\frac{1}{4}h_0 k\right)^{2|m|}}{(|m|!)^2} \frac{\cos\theta}{\cos\theta'}(\cos\theta + \cos\theta')^{2|m|}, \qquad (29)$$

where we assumed that scattering occurs along the x axis. Therefore, the angular component of the probability of transition $P_\theta(\theta, \theta', x)$ as given by Eq. (22) is equal to

$$P_\theta(\theta, \theta', x) = \frac{\cos\theta}{\cos\theta'} \sum_{m=-\infty}^{\infty} \frac{\left(\frac{1}{4}h_0 k\right)^{2|m|}}{(|m|!)^2} \cdot (\cos\theta + \cos\theta')^{2|m|} e^{i\frac{2\pi m x}{L_0}}. \qquad (30)$$

Using κ to denote the following coefficient:

$$\kappa = \frac{1}{4}h_0 k = \frac{\pi}{2} m_p v_0 \frac{h_0}{h}, \qquad (31)$$

we can rewrite the expression given by Eq. (30) in a form which eliminates absolute values of the summation index m,

$$P_\theta(\theta, \theta', x) = \frac{\cos\theta}{\cos\theta'}\left(2\sum_{m=1}^{\infty} \frac{\kappa^{2m}}{(m!)^2}(\cos\theta' + \cos\theta)^{2m}\cos\left(\frac{2\pi m}{L_0}x\right) + 1\right). \qquad (32)$$

This can be further simplified to

$$P_\theta(\theta, \theta', x) = \frac{1}{2}\frac{\cos\theta}{\cos\theta'}\left[I_0\left(2\kappa(\cos\theta + \cos\theta')e^{i\frac{\pi x}{L_0}}\right) + I_0\left(2\kappa(\cos\theta + \cos\theta')e^{-i\frac{\pi x}{L_0}}\right) - 2\right]. \qquad (33)$$

Here, I_0 is the zeroth-order modified Bessel function of the first kind. While this expression is the angular probability density of scattering in its most compact possible form, we will in further instances refer to the form given by Eq. (32).

III. DETERMINING THE COMPLETE PROBABILITY DENSITY FUNCTION

This part of the paper presents the methods which we use to determine the expression for the complete probability density function given in Eq. (17).

Function $f^-(v'_i)$, which appears in Eq. (17), is a product of two separate functions

$$f^-(v'_i) = f_0(v'_0) f_{\text{inc}}(\theta'), \qquad (34)$$

where we used primed variables to denote that they pertain to particles entering the region [velocity transformations as given by Eq. (20) are also valid for primed variables]. Quantities, which appear in the expression, are shown in Fig. 4. Function $f_{\text{inc}}(\theta')$ is the probability density function of a particle entering the region at a certain angle θ' relative to the y axis. We assume it to be equal to $f_{\text{inc}}(\theta) = \frac{\pi}{2}\cos\theta'$, where $\theta' \in [\frac{\pi}{2}, \frac{3\pi}{2}]$ (the factor of $\frac{\pi}{2}$ is present for purposes of normalization). The functional form of f_{inc} is justified by observing the fact that if a particle undergoes a collision with another particle right at the upper bound of the region near the surface, it will certainly enter the

region if its velocity component points straight downward, meaning that $\theta' = \pi$. Conversely, the particle will certainly not enter the region if the angle θ' is either $\theta' = \frac{\pi}{2}$ or $\theta' = \frac{3\pi}{2}$ (Fig. 4 should serve as an additional graphical explanation of this fact). With function f_0 given by Eq. (15), we can assert that function $f^-(v'_i)$ is therefore equal to

$$f^-(v'_i, y_{\text{Kn}}) = \frac{\pi}{2} n\left(\frac{m_p}{2\pi k_B T}\right)^{\frac{3}{2}} e^{-\frac{m_p(u_0'^2 + u_z'^2)}{2 k_B T}} \cos\theta'. \qquad (35)$$

Determining f^+ in Eq. (17) is achieved by integrating the product of f^- and the full conditional probability density function P, which determines the probability of particles with some initial velocity, described by parameters u'_0, θ', and u'_z, scattering off the surface with a final velocity determined by u_0, θ, and u_z. This is given by the expression

$$f^+(u_0, \theta, u_z, x, y_{\text{Kn}}) = \iiint_{v'_y < 0} f^-(u'_0, \theta', u'_z) \\ \cdot P(u_0, u'_0, \theta, \theta', u_z, u'_z, x)\, du'_0\, d\theta'\, du_z, \qquad (36)$$

where we integrate over velocities corresponding to particles traveling toward the surface. Conditional probability density $P(u_0, u'_0, \theta, \theta', u'_z, u_z, x)$ can be written as a product of three separate functions

$$P(u_0, u'_0, \theta, \theta', u_z, u'_z, x) = \frac{1}{\pi J} P_{u_0}(u_0, u'_0) P_\theta(\theta, \theta', x) P_{u_z}(u_z, u'_z), \qquad (37)$$

where J is the Jacobian from Eq. (21). Because momentum and kinetic energy are conserved when particles scatter from the surface elastically, functions $P_{u_0}(u_0, u'_0)$ and $P_{u_z}(u_z, u'_z)$ are equal to

$$\begin{aligned} P_{u_0}(u_0, u'_0) &= \delta(u_0 - u'_0), \\ P_{u_z}(u_z, u'_z) &= \delta(u_z - u'_z), \end{aligned} \qquad (38)$$

while the angular probability density of scattering is given by Eq. (32). The full conditional probability density function from Eq. (37) is therefore given by

$$P(u_0, u'_0, \theta, \theta', u_z, u'_z, x, y_{\text{Kn}}) \\ = \frac{1}{\pi J}\delta(u_0 - u'_0)\,\delta(u_z - u'_z) \\ \cdot \frac{\cos\theta}{\cos\theta'}\left(2\sum_{m=1}^{\infty}\left(\frac{\kappa^m}{m!}\right)^2(\cos\theta' + \cos\theta)^{2m} e^{i\frac{2\pi m}{L_0}x} + 1\right) \\ = \frac{2}{\pi J}\delta(u_0 - u'_0)\,\delta(u_z - u'_z) \\ \cdot \frac{\cos\theta}{\cos\theta'}\left[I_0(2\,\kappa\,e^{i\frac{\pi}{L_0}x}(\cos\theta + \cos\theta')) - 1\right], \qquad (39)$$

where I_0 is the zeroth-order modified Bessel function of the first kind. Coefficient denoted by κ in the expression above is in accordance with Eq. (32) equal to

$$\kappa = \frac{\pi}{2}\frac{h_0 m_p}{h}\sqrt{u_0'^2 + u_z'^2} = c_1\sqrt{u_0'^2 + u_z'^2}, \qquad (40)$$

where the magnitude of velocity relative to the surface is defined in accordance with Eq. (19), while Fig. 4 can serve as additional

explanation. Primed variables u_0' and u_z' appear in the expression for κ because it pertains to incident particles. In order to solve the integral in Eq. (36), we need to introduce the following transformation of variables: $\theta' \rightarrow \pi - \theta'$ in Eq. (35). Its purpose is to ensure that the way we defined angle θ' in this expression conforms to the definition of the incident and scattering angles, which appear in the angular probability density function of scattering, Eq. (32), and are also shown in Fig. 4. This transformation also requires us to modify the range of integration over θ', which becomes $\theta' \in [\frac{\pi}{2}, -\frac{\pi}{2}]$. Integration ranges of u_0' and u_z' are equal to $u_0' \in [w, \infty)$ and $u_z' \in (-\infty, \infty)$. Accounting for the fact that $\cos(\pi - \theta') = -\cos \theta'$, we can rewrite Eq. (36) as

$$f^+(u_0, \theta, u_z, x, y_{Kn}) = \frac{1}{2} n \left(\frac{m_P}{2\pi k_B T}\right)^{\frac{3}{2}} e^{-\frac{m_P(u_0^2 + u_z^2)}{2k_B T}}$$
$$\times \cos \theta (\pi + 2\mathscr{F}_0(u_0, \theta, u_z, x)), \quad (41)$$

where the function $\mathscr{F}_0$ is given by the expression

$$\mathscr{F}_0(u_0, \theta, u_z, x) = \pi \sum_{m=1}^{\infty} \frac{(c_1 u_0)^{2m}}{(m!)^2} \left[\sum_{k=0}^{2m} \binom{2m}{k} \frac{\cos^k \theta}{2^{2m-k}} \right.$$
$$\times \sum_{n=0}^{2m-k} \binom{2m-k}{n} \text{sinc}\left(\frac{\pi}{2}(2(n-m)+k)\right) \right]$$
$$\times \cos\left(\frac{2\pi m}{L_0} x\right). \quad (42)$$

The definition of c_1 is evident from Eq. (41). Two important steps in solving the integral over possible velocities as given by Eq. (36), which results in Eqs. (41) and (42), are presented by Eqs. (A1) and (A2) in the Appendix. The full velocity probability density function of particles moving through the Knudsen region as defined by (17) is therefore equal to

$$f(u_0, \theta, u_z, x, y_{Kn}) = \frac{\pi}{4} n \left(\frac{m_P}{2\pi k_B T}\right)^{\frac{3}{2}} e^{-\frac{m_P(u_0^2 + u_z^2)}{2k_B T}} \cos \theta (1 - \text{sgn}(u_0 \cos \theta))$$
$$+ \frac{1}{4} n \left(\frac{m_P}{2\pi k_B T}\right)^{\frac{3}{2}} e^{-\frac{m_P(u_0^2 + u_z^2)}{2k_B T}}$$
$$\times \cos \theta (\pi + 2\mathscr{F}_0(u_0, u_z, \theta, x))$$
$$\times (1 + \text{sgn}(u_0 \cos \theta)). \quad (43)$$

We abandon the prime notation pertaining to incident particles at this point in the text.

IV. VELOCITY COMPONENTS IN THE KNUDSEN LAYER

This section of the paper deals with the fluid velocity components in the Knudsen layer and demonstrate the methodology used to obtain expressions determining these quantities. Velocity components are determined by statistically averaging particle velocities using the method described by Eq. (8), while the probability density function is taken to be given by Eq. (43). At this point, it should be noted that because the probability density function contains spatial dependence on the length scale L_0, which is significantly smaller than the minimum length scale L_{min} at which the assumption of continuum holds true, resulting statistical averages will correspond to mesoscopic quantities.

Statistical average of some velocity component is equal to

$$v_i = \frac{1}{n} \int_{-\infty}^{\infty} \int_{-\infty}^{\infty} \int_{-\infty}^{\infty} v_i f(r_i, v_i, t) \, dv_i \, dv_j \, dv_k, \quad (44)$$

where we integrate over all possible velocities. In accordance with this expression, we can determine the statistical average of the tangential velocity component to be equal to

$$v_x(x, y_{Kn}, w) = v_x = u_0 \sin(\theta) + w$$
$$= \frac{1}{n} \left[\iiint_{u_y < 0} u_0 \sin \theta f^-(-u_0) \, du \, d\theta \, du_z \right.$$
$$+ \iiint_{u_y > 0} u_0 \sin \theta f^+(-u_0) \, du \, d\theta \, du_z \right]$$
$$+ \frac{w}{n} \left[\iiint_{u_y < 0} f^-(-u_0) \, du_0 \, d\theta \, du_z \right.$$
$$+ \iiint_{u_y > 0} f^+(-u_0) \, du_0 \, d\theta du_z \right]. \quad (45)$$

The expression above contains four different multivariate integrals, which are evaluated over intervals corresponding to conditions $v_y < 0$ (particles moving toward the surface) and $v_y > 0$ (particles being scattered off the surface). Integration ranges, which correspond to the condition $u_y < 0$, are as follows: $[\frac{\pi}{2}, \frac{3\pi}{2}]$ for θ, $[w, \infty)$ for u_0 and $[-\infty, \infty]$ for u_z, while ranges that correspond to condition $u_y > 0$ are as follows: $[\frac{\pi}{2}, -\frac{\pi}{2}]$ for θ, $[w, \infty)$ for u_0 and $[-\infty, \infty]$ for u_z.

The first and the second terms in Eq. (45) are equal to

$$\iiint_{u_y < 0} u_0 \sin \theta f^-(u_0, \theta, u_z)(-u_0) \, du_0 \, d\theta \, du_z = 0 \quad (46)$$

and

$$\iiint_{u_y > 0} u_0 \sin \theta f^+(u_0, \theta, u_z)(-u_0) \, du_0 \, d\theta \, du_z = 0, \quad (47)$$

while the third term is equal to

$$\iiint_{u_y < 0} f^-(u_0, \theta, u_z)(-u_0) \, du_0 \, d\theta \, du_z = \frac{1}{2} n e^{-\frac{m_P w^2}{2k_B T}}. \quad (48)$$

The fourth term is given by

$$\iiint_{u_y > 0} f^+(u_0, \theta, u_z, x)(-u_0) \, du_0 \, d\theta \, du_z$$
$$= -\frac{1}{2} n \left(\frac{m_P}{2\pi k_B T}\right)^{\frac{3}{2}} \int_{-\infty}^{\infty} e^{-\frac{m_P u_z^2}{2k_B T}} \, du_z$$
$$\cdot \int_{\frac{\pi}{2}}^{-\frac{\pi}{2}} \int_w^{\infty} u_0 e^{-\frac{m_P u_0^2}{2k_B T}} \cos \theta (\pi + 2\mathscr{F}_0(u_0, \theta, u_z, x)) \, du_0 \, d\theta, \quad (49)$$

where we can observe that the expression in parentheses itself consists of two terms. The result of integrating over the first of two terms is equal to Eq. (48), while the result of integrating over the second is equal to

$$-\frac{m_P}{2\pi k_B T} n \int_{\frac{\pi}{2}}^{-\frac{\pi}{2}} \int_w^{\infty} u_0 e^{-\frac{m_P u_0^2}{2k_B T}} \cos \theta \mathscr{F}_0(u_0, \theta, 0, x) \, du_0 \, d\theta = \frac{\sqrt{\pi}}{2} \mathscr{F}_2(x, w).$$
$$(50)$$

In determining the expression above, we decided to neglect the dependence of κ on the lateral velocity component u_z, which can be expressed as $\sqrt{u_0^2 + u_z^2} \approx u_0$. This is valid because we are dealing with a quasi-two-dimensional system where we can neglect the influence of motion in the z-direction, and solutions which are based on this simplification differ from solutions, which are not only in a multiplicative factor. Function $\mathscr{F}_2$, which appears in Eq. (50), is given by

$$
\begin{aligned}
\mathscr{F}_2(x, w) = &\sum_{m=1}^{\infty} \frac{\left(\frac{c_1^2}{c_2}\right)^m}{(m!)^2} \, \Gamma\left(m+1, \frac{m_{\mathrm{p}} w^2}{2k_{\mathrm{B}} T}\right) \\
&\times \left[\sum_{k=0}^{2m} \binom{2m}{k} 2^{k-2m} \frac{\Gamma\left(\frac{k+2}{2}\right)}{\Gamma\left(\frac{k+3}{2}\right)} \sum_{n=0}^{2m-k} \binom{2m-k}{n}\right. \\
&\left.\times \operatorname{sinc}\left(\frac{\pi}{2}(2(n-m)+k)\right)\right] \cos\left(\frac{2\pi m}{L_0} x\right),
\end{aligned}
$$
(51)

where c_2 represents the constant factor

$$
c_2 = \frac{m_{\mathrm{p}}}{2k_{\mathrm{B}} T}.
$$
(52)

Tangential velocity v_x is therefore equal to

$$
\mathrm{v}_x(x, y_{\mathrm{Kn}}, w) = w\left(e^{-\frac{m_{\mathrm{p}} w^2}{2k_{\mathrm{B}} T}} + \frac{\sqrt{\pi}}{2} \mathscr{F}_2(x, w)\right).
$$
(53)

Statistical average of the normal velocity component is equal to

$$
\begin{aligned}
\mathrm{v}_y(x, y_{\mathrm{Kn}}, w) = \langle v_y \rangle = &\langle u_0 \cos\theta \rangle \\
= \frac{1}{n}\left[\iiint_{v_y<0} u_0 \cos\theta f^-(-u_0)\, du_0\, d\theta\, du_z\right. \\
&\left.+ \iiint_{v_y>0} u_0 \cos\theta f^+(-u_0)\, du_0\, d\theta\, du_z\right],
\end{aligned}
$$
(54)

and like before, it consists of several parts. The first part is equal to

$$
\iiint_{v_y<0} u_0 \cos\theta f^-(-u_0)\, du_0\, d\theta\, du_z = -n\frac{m_{\mathrm{p}}}{8k_{\mathrm{B}} T} I_1(w),
$$
(55)

where $I_1(w)$ is the integral over u_0 and θ, while the second part is equal to

$$
\begin{aligned}
&\iiint_{v_y>0} u_0 \cos\theta f^+(-u_0)\, du_0\, d\theta\, du_z \\
&= -\frac{1}{2} n\left(\frac{m_{\mathrm{p}}}{2\pi k_{\mathrm{B}} T}\right)^{\frac{3}{2}} \int_{-\infty}^{\infty} e^{-\frac{m_{\mathrm{p}} u_z^2}{2k_{\mathrm{B}} T}}\, du_z \\
&\quad \cdot \int_{\frac{\pi}{2}}^{-\frac{\pi}{2}} \int_{w}^{\infty} u_0^2 e^{-\frac{m_{\mathrm{p}} u_0^2}{2k_{\mathrm{B}} T}} \cos^2\theta\, (\pi + 2\mathscr{F}_0(u_0, \theta, x))\, du_0\, d\theta \\
&= n\frac{m_{\mathrm{p}}}{8k_{\mathrm{B}} T} I_1(w) + \frac{1}{2} n\sqrt{\frac{2k_{\mathrm{B}} T}{m_{\mathrm{p}}}} \mathscr{F}_1(x, w).
\end{aligned}
$$
(56)

Function $\mathscr{F}_1(x, w)$, which appears in Eq. (56), is given by

$$
\begin{aligned}
\mathscr{F}_1(x, w) = &\sum_{m=1}^{\infty} \frac{\left(\frac{c_1^2}{c_2}\right)^m}{(m!)^2} \, \Gamma\left(m+\frac{3}{2}, \frac{m_{\mathrm{p}} w^2}{2k_{\mathrm{B}} T}\right) \\
&\times \left[\sum_{k=0}^{2m} \binom{2m}{k} 2^{k-2m} \frac{\Gamma\left(\frac{k+3}{2}\right)}{\Gamma\left(\frac{k+4}{2}\right)} \sum_{n=0}^{2m-k} \binom{2m-k}{n}\right. \\
&\left.\times \operatorname{sinc}\left(\frac{\pi}{2}(2(n-m)+k)\right)\right] \cos\left(\frac{2\pi m}{L_0} x\right).
\end{aligned}
$$
(57)

As we can see, the expression given by Eq. (55) and the second term in Eq. (56) cancel each other out, which means that normal velocity v_y is therefore equal to

$$
\mathrm{v}_y(x, y_{\mathrm{Kn}}, w) = \frac{\pi}{4} v_{\mathrm{th}} \mathscr{F}_1(x, w),
$$
(58)

where we used v_{th} to denote the fluid thermal velocity, which is defined as the mean of the velocity magnitude as

$$
v_{\mathrm{th}} = \sqrt{\frac{8k_{\mathrm{B}} T}{\pi m_{\mathrm{p}}}}.
$$
(59)

Mathematical expressions and equalities, which can serve as additional explanation of the derivations of Eqs. (53) and (58), are shown in the Appendix by Eqs. (A3)–(A5).

V. STRESS TENSOR COMPONENTS IN THE KNUDSEN LAYER

This section of the paper deals with stress tensor components in the Knudsen layer using the same method of statistical averaging, given by Eqs. (8) and (17), as in Sec. IV.

Stress tensor component σ_{ij} is obtained by statistically averaging the flux of the ith component of momentum relative to the direction parallel to the jth component of velocity. This can be expressed as

$$
\begin{aligned}
\sigma_{ij} &= \langle m_{\mathrm{p}}(v_i - \mathrm{v}_i)(v_j - \mathrm{v}_j)\rangle \\
&= \int_{-\infty}^{\infty}\int_{-\infty}^{\infty}\int_{-\infty}^{\infty} m_{\mathrm{p}}(v_i - \mathrm{v}_i)(v_j - \mathrm{v}_j)\, n(r_i) f(r_i, v_i, t)\, dv_i\, dv_j\, dv_k,
\end{aligned}
$$
(60)

where we integrate over all possible velocities. We first attend diagonal stress tensor components σ_{ii}, which are obtained as

$$
\begin{aligned}
\sigma_{ii} &= \langle m_{\mathrm{p}}(v_i - \mathrm{v}_i)(v_i - \mathrm{v}_i)\rangle \\
&= m_{\mathrm{p}}\langle (v_i^2 - 2v_i\mathrm{v}_i + \mathrm{v}_i^2)\rangle \\
&= m_{\mathrm{p}}\left(\langle v_i^2 \rangle - n\mathrm{v}_i^2\right).
\end{aligned}
$$
(61)

Since this identity holds true for all three diagonal stress tensor components, it is simple to observe that we only need to determine statistical averages of the squares of velocity components v_i^2, while v_i is the statistical average of a velocity component given by Eq. (44). Stress tensor component σ_{xx} is equal to

$$
\sigma_{xx}(x, y_{\mathrm{Kn}}, w) = m_{\mathrm{p}}\left(\langle v_x^2 \rangle - n\mathrm{v}_x^2\right),
$$
(62)

and the statistical average of v_x^2 is equal to

$$\langle v_x^2 \rangle = \langle (u_0 \sin\theta + w)^2 \rangle = \langle u_0^2 \sin^2\theta + 2wu_0 \sin\theta + w^2 \rangle. \quad (63)$$

The second term in statistical average above is equal to zero, as can be deduced from Eq. (A4), while the third term is equal to

$$\langle w^2 \rangle = w^2 \left(e^{-\frac{m_p w^2}{2k_B T}} + \frac{\sqrt{\pi}}{2} \mathscr{F}_2(x,w) \right). \quad (64)$$

The first term in Eq. (63) can be evaluated as

$$\langle u_0^2 \sin^2\theta \rangle = \iiint_{v_y<0} u_0^2 \sin^2\theta f^-(-u_0) \, du_0 \, d\theta \, du_z$$
$$+ \iiint_{v_y>0} u_0^2 \sin^2\theta f^+(-u_0) \, du_0 \, d\theta \, du_z. \quad (65)$$

The two terms in the previous expression are equal to

$$\iiint_{v_y<0} u_0^2 \sin^2\theta f^-(-u_0) \, du_0 \, d\theta \, du_z$$
$$= \frac{1}{3} n \frac{k_B T}{m_p} e^{-\frac{m_p w^2}{2k_B T}} \left(1 + \frac{m_p w^2}{2k_B T} \right) \quad (66)$$

and

$$\iiint_{v_y>0} u_0^2 \sin^2\theta f^+(-u_0) \, du_0 \, d\theta \, du_z$$
$$= n \frac{k_B T}{m_p} \left(\frac{1}{3} e^{-\frac{m_p w^2}{2k_B T}} \left(1 + \frac{m_p w^2}{2k_B T} \right) + \frac{\sqrt{\pi}}{2} \mathscr{F}_3(x,w) \right), \quad (67)$$

where the function $\mathscr{F}_3$ is equal to

$$\mathscr{F}_3(x,w) = \sum_{m=1}^{\infty} \frac{\left(\frac{c_1^2}{c_2}\right)^m}{(m!)^2} \Gamma\left(m+2, \frac{m_p w^2}{2k_B T}\right)$$
$$\times \left[\sum_{k=0}^{2m} \binom{2m}{k} 2^{k-2m} \frac{\Gamma\left(\frac{k+2}{2}\right)}{\Gamma\left(\frac{k+5}{2}\right)} \sum_{n=0}^{2m-k} \binom{2m-k}{n} \right.$$
$$\left. \times \operatorname{sinc}\left(\frac{\pi}{2}(2(n-m)+k)\right) \right] \cos\left(\frac{2\pi m}{L_0}x\right). \quad (68)$$

Combining the terms, given by Eqs. (53), (64), (66), and (67) in the proper manner, we arrive at the expression for the stress tensor component σ_{xx}, which is equal to

$$\sigma_{xx}(x, y_{\mathrm{Kn}}, w) = p_0 \left[\frac{2}{3} e^{-\frac{m_p w^2}{2k_B T}} \left(1 + \frac{m_p w^2}{2k_B T} \right) + \frac{\sqrt{\pi}}{2} \mathscr{F}_3(x,w) \right]$$
$$+ \rho w^2 \left[\left(e^{-\frac{m_p w^2}{2k_B T}} + \frac{\sqrt{\pi}}{2} \mathscr{F}_2(x,w) \right) \right.$$
$$\left. - \left(e^{-\frac{m_p w^2}{2k_B T}} + \frac{\sqrt{\pi}}{2} \mathscr{F}_2(x,w) \right)^2 \right], \quad (69)$$

where p_0 is the thermodynamically defined pressure as given by the ideal gas law $p_0 = n k_B T$.

Stress tensor component σ_{yy} is given by

$$\sigma_{yy} = m_p \left(\langle v_y^2 \rangle - n v_y^2 \right), \quad (70)$$

and the statistical average of v_y^2 is equal to

$$\langle v_y^2 \rangle = \langle u_0^2 \cos^2\theta \rangle$$
$$= \iiint_{v_y<0} u_0^2 \cos^2\theta f^-(-u_0) \, du_0 \, d\theta \, du_z$$
$$+ \iiint_{v_y>0} u_0^2 \cos^2\theta f^+(-u_0) \, du_0 \, d\theta \, du_z. \quad (71)$$

The two terms in the previous equation are equal to

$$\iiint_{v_y<0} u_0^2 \cos^2\theta f^-(-u_0) \, du_0 \, d\theta \, du_z$$
$$= \frac{2}{3} n \frac{k_B T}{m_p} e^{-\frac{m_p w^2}{2k_B T}} \left(1 + \frac{m_p w^2}{2k_B T} \right) \quad (72)$$

and

$$\iiint_{v_y>0} u_0^2 \cos^2\theta f^+(-u_0) \, du_0 \, d\theta \, du_z$$
$$= \frac{2}{3} n \frac{k_B T}{m_p} e^{-\frac{m_p w^2}{2k_B T}} \left(1 + \frac{m_p w^2}{2k_B T} \right) + \sqrt{\pi} n \frac{k_B T}{m_p} \mathscr{F}_4(x,w), \quad (73)$$

where the function $\mathscr{F}_4$ equals to

$$\mathscr{F}_4(x,w) = \sum_{m=1}^{\infty} \frac{\left(\frac{c_1^2}{c_2}\right)^m}{(m!)^2} \Gamma\left(m+2, \frac{m_p w^2}{2k_B T}\right)$$
$$\times \left[\sum_{k=0}^{2m} \binom{2m}{k} 2^{k-2m} \frac{\Gamma\left(\frac{k+4}{2}\right)}{\Gamma\left(\frac{k+5}{2}\right)} \sum_{n=0}^{2m-k} \binom{2m-k}{n} \right.$$
$$\left. \times \operatorname{sinc}\left(\frac{\pi}{2}(2(n-m)+k)\right) \right] \cos\left(\frac{2\pi m}{L_0}x\right). \quad (74)$$

Combining the terms, given by Eqs. (58), (72), and (73), we obtain the expression for the stress tensor component σ_{yy}, which equals

$$\sigma_{yy}(x, y_{\mathrm{Kn}}, w) = p_0 \left[\frac{4}{3} e^{-\frac{m_p w^2}{2k_B T}} \left(1 + \frac{m_p w^2}{2k_B T} \right) + \sqrt{\pi} \mathscr{F}_4(x,w) \right]$$
$$- \left(\frac{\pi}{4} \right)^2 \rho v_{\mathrm{th}}^2 \mathscr{F}_1^2(x,w). \quad (75)$$

Stress tensor component σ_{zz} is accordingly equal to

$$\sigma_{zz}(x, y_{\mathrm{Kn}}, w) = m_p (\langle v_z^2 \rangle - n v_z^2). \quad (76)$$

Because the statistical average of v_z is zero as we assumed no net flow in the z-direction, we only need to evaluate $\langle v_z^2 \rangle$ in order to obtain Eq. (76), which we do by solving

$$\langle v_z^2 \rangle = \langle u_z^2 \rangle$$
$$= \iiint_{v_y<0} u_z^2 f^- (-u_0)\, du_0\, d\theta\, du_z$$
$$+ \iiint_{v_y>0} u_z^2 f^+ (-u_0)\, du_0\, d\theta\, du_z. \tag{77}$$

The two terms in the previous equation are equal to

$$\iiint_{v_y<0} u_z^2 f^- (-u_0)\, du_0\, d\theta\, du_z = \frac{1}{2} n \frac{k_B T}{m_p} e^{-\frac{m_p w^2}{2k_B T}} \tag{78}$$

and

$$\iiint_{v_y>0} u_z^2 f^+ (-u_0)\, du_0\, d\theta\, du_z$$
$$= \frac{1}{2} n \frac{k_B T}{m_p} e^{-\frac{m_p w^2}{2k_B T}} + \frac{\sqrt{\pi}}{2} n \frac{k_B T}{m_p} \mathscr{F}_2(x, w). \tag{79}$$

Combining the terms, given by Eqs. (78) and (79), we arrive at the expression for the stress tensor component σ_{zz}, which is equal to

$$\sigma_{zz}(x, y_{Kn}, w) = p_0 \left(e^{-\frac{m_p w^2}{2k_B T}} + \frac{\sqrt{\pi}}{2} \mathscr{F}_2(x, w) \right). \tag{80}$$

Expressions (69), (75), and (80) can be combined to obtain an expression for static pressure p as a function of x and w in the following way:

$$p(x, y_{Kn}, w) = p_0 \left[e^{-\frac{m_p w^2}{2k_B T}} \left(1 + \frac{m_p w^2}{3k_B T} \right) \right.$$
$$+ \frac{\sqrt{\pi}}{3} \left(\frac{1}{2} \mathscr{F}_3(x, w) + \mathscr{F}_4(x, w) + \frac{1}{2} \mathscr{F}_2(x, w) \right)$$
$$- \frac{\pi}{6} \mathscr{F}_1^2(x, w) \right] + \frac{1}{3} \rho w^2 \left[\left(e^{-\frac{m_p w^2}{2k_B T}} + \frac{\sqrt{\pi}}{2} \mathscr{F}_2(x, w) \right) \right.$$
$$\left. - \left(e^{-\frac{m_p w^2}{2k_B T}} + \frac{\sqrt{\pi}}{2} \mathscr{F}_2(x, w) \right)^2 \right], \tag{81}$$

where functions $\mathscr{F}_1$, $\mathscr{F}_2$, $\mathscr{F}_3$, and $\mathscr{F}_4$ are given by Eqs. (57), (51), (68), and (74).

We now turn our attention to non-diagonal components of the stress tensor components of the stress tensor. The shear stress present is in our case described by the component σ_{yx}, which is in accordance with Eq. (60) equal to

$$\sigma_{yx} = m_p \langle (v_x - v_x)(v_y - v_y) \rangle = m_p (\langle v_x v_y \rangle - n v_x v_y). \tag{82}$$

Evaluating the statistical average of the product $v_x v_y$ gives us

$$\langle v_x v_y \rangle = \langle (u_0 \sin\theta + w) u_0 \cos\theta \rangle$$
$$= \left\langle \frac{1}{2} u_0^2 \sin(2\theta) \right\rangle + w \langle u_0 \cos\theta \rangle$$
$$= n w v_y(x, y_{Kn}, w). \tag{83}$$

The first term in the expression above is zero, which can be verified by examining Eq. (A4), while the second term is equal to the product of wall velocity w and the statistical average of normal velocity component v_y. The shear stress given by σ_{yx} is accordingly given by

$$\sigma_{yx}(x, y_{Kn}, w) = \frac{\pi}{4} \rho v_{th} w \mathscr{F}_1(x, w) \cdot \left(1 - e^{-\frac{m_p w^2}{2k_B T}} - \frac{\sqrt{\pi}}{2} \mathscr{F}_2(x, w) \right), \tag{84}$$

where ρ is density (product of particle mass m_p and number density n), while thermal velocity is defined by Eq. (59). Functions $\mathscr{F}_1$ and $\mathscr{F}_2$ are given by Eqs. (57) and (51). Mathematical expressions and equalities, which can serve as additional explanation of the derivations of Eqs. (69), (75), (80), (81), and (84), are shown in the Appendix by Eqs. (A3), (A5), and (A6).

VI. SPATIAL AVERAGES OF QUANTITIES IN THE KNUDSEN LAYER

In this section, we demonstrate how to obtain spatial averages of quantities in the Knudsen layer along the direction defined by the x axis. Spatial averages of quantities can be determined by evaluating the following integral:

$$\bar{\psi} = \frac{1}{x_0} \int_0^{x_0} \psi(x) dx, \tag{85}$$

where x_0 approaches infinity: $x_0 \to \infty$. If we express functions $\mathscr{F}_{1a}$, $\mathscr{F}_{2a}$, $\mathscr{F}_{3a}$, and $\mathscr{F}_{4a}$, which determine the quantities of interest in the Knudsen layer as trigonometric series in the form of

$$f(x, w) = \sum_{m=1}^{\infty} f_m(w) \cos\left(\frac{2\pi m}{L_0} x \right) \tag{86}$$

or

$$g(x, w) = \sum_{m=1}^{\infty} g_m(w) \cos\left(\frac{2\pi m}{L_0} x \right), \tag{87}$$

we can notice that spatial averages of such functions are equal to zero

$$\overline{f(w)} = \lim_{x_0 \to \infty} \frac{1}{x_0} \int_0^{x_0} \sum_{m=1}^{\infty} f_m(w) \cos\left(\frac{2\pi m}{L_0} x \right) dx$$
$$= \lim_{x_0 \to \infty} \frac{1}{x_0} \sum_{m=1}^{\infty} f_m(w) \int_0^{x_0} \cos\left(\frac{2\pi m}{L_0} x \right) dx$$
$$= \frac{L_0}{2\pi} \sum_{m=1}^{\infty} f_m(w) \left(\lim_{x_0 \to \infty} \frac{1}{x_0} \sin\left(2\pi m \frac{x_0}{L_0} \right) \right)$$
$$= 0. \tag{88}$$

Because we are evaluating spatial averages of functions, which are periodic on the interval $[0, \infty]$, we do not need to evaluate the limit of the expression. Furthermore, we can replace the interval of integration by $[-\frac{1}{2} L_0, \frac{1}{2} L_0]$ if $\psi(x)$ is periodic on this interval. It can also be shown that spatial averages of products of functions, which, in general, have the forms given by Eqs. (86) and (87) are equal to

$$\overline{f(w)g(w)} = \frac{1}{L_0} \int_{-\frac{L_0}{2}}^{\frac{L_0}{2}} f(x, w) g(x, w)\, dx = \frac{1}{2} \sum_{m=1}^{\infty} f_m(w) g_m(w). \tag{89}$$

A short proof of the formula presented above is given by Eq. (A7). An immediate consequence of identity (89) is the following expression for the spatial average of a square of some function of the form given by Eq. (86), which equals

$$\overline{f^2}(w) = \frac{1}{L_0} \int_{-\frac{L_0}{2}}^{\frac{L_0}{2}} f^2(x, w) \, dx = \frac{1}{2} \sum_{m=1}^{\infty} f_m^2(w). \tag{90}$$

According to Eq. (89), we can show that the spatial averages of velocity components v_x and v_y in the Knudsen layer, given by Eqs. (53) and (58), are therefore equal to

$$\bar{v}_x(y_{Kn}, w) = \frac{1}{L_0} \int_{-\frac{L_0}{2}}^{\frac{L_0}{2}} v_x(x, w) \, dx$$
$$= w e^{-\frac{m_p w^2}{2 k_B T}} \tag{91}$$

and

$$\bar{v}_y(y_{Kn}, w) = \frac{1}{L_0} \int_{-\frac{L_0}{2}}^{\frac{L_0}{2}} v_y(x, w) \, dx$$
$$= 0. \tag{92}$$

We can take similar steps to determine spatial averages of the stress tensor components pertaining to the Knudsen layer. Functions $\mathscr{F}_1$ and $\mathscr{F}_2$ can be expressed in the form of trigonometric series, given by

$$\mathscr{F}_1(x, w) = \sum_{m=1}^{\infty} a_m(w) \cos\left(\frac{2\pi m}{L_0} x\right) \tag{93}$$

and

$$\mathscr{F}_2(x, w) = \sum_{m=1}^{\infty} b_m(w) \cos\left(\frac{2\pi m}{L_0} x\right), \tag{94}$$

where coefficients a_m and b_m are equal to

$$a_m(w) = \frac{\left(\frac{c_1^2}{c_2}\right)^m}{(m!)^2} \Gamma\left(m + \frac{3}{2}, \frac{m_p w^2}{2 k_B T}\right)$$
$$\cdot \left[\sum_{k=0}^{2m} \binom{2m}{k} 2^{k-2m} \frac{\Gamma\left(\frac{k+3}{2}\right)}{\Gamma\left(\frac{k+4}{2}\right)}\right.$$
$$\left.\cdot \sum_{n=0}^{2m-k} \binom{2m-k}{n} \mathrm{sinc}\left(\frac{\pi}{2}(2(n-m)+k)\right)\right] \tag{95}$$

and

$$b_m(w) = \frac{\left(\frac{c_1^2}{c_2}\right)^m}{(m!)^2} \Gamma\left(m + 1, \frac{m_p w^2}{2 k_B T}\right)$$
$$\cdot \left[\sum_{k=0}^{2m} \binom{2m}{k} 2^{k-2m} \frac{\Gamma\left(\frac{k+2}{2}\right)}{\Gamma\left(\frac{k+3}{2}\right)}\right.$$
$$\left.\cdot \sum_{n=0}^{2m-k} \binom{2m-k}{n} \mathrm{sinc}\left(\frac{\pi}{2}(2(n-m)+k)\right)\right]. \tag{96}$$

Consequently, by referring to the equality given by Eq. (90), averages of stress tensor elements σ_{xx}, σ_{yy}, and σ_{zz} can be expressed as

$$\bar{\sigma}_{xx}(y_{Kn}, w) = \frac{1}{L_0} \int_{-\frac{L_0}{2}}^{\frac{L_0}{2}} \sigma_{xx}(x, y_{Kn}, w) \, dx$$
$$= \frac{2}{3} p_0 e^{-\frac{m_p w^2}{2 k_B T}} \left(1 + \frac{m_p w^2}{2 k_B T}\right)$$
$$+ \rho w^2 \left(e^{-\frac{m_p w^2}{2 k_B T}} - e^{-\frac{m_p w^2}{k_B T}} - \frac{\pi}{8} \sum_{m=1}^{\infty} b_m^2(w)\right), \tag{97}$$

$$\bar{\sigma}_{yy}(y_{Kn}, w) = \frac{1}{L_0} \int_{-\frac{L_0}{2}}^{\frac{L_0}{2}} \sigma_{yy}(x, y_{Kn}, w) \, dx$$
$$= p_0 \left(\frac{4}{3} e^{-\frac{m_p w^2}{2 k_B T}} \left(1 + \frac{m_p w^2}{2 k_B T}\right) - \frac{\pi}{4} \sum_{m=1}^{\infty} a_m^2(w)\right), \tag{98}$$

and

$$\bar{\sigma}_{zz}(y_{Kn}, w) = \frac{1}{L_0} \int_{-\frac{L_0}{2}}^{\frac{L_0}{2}} \sigma_{zz}(x, y_{Kn}, w) \, dx = p_0 e^{-\frac{m_p w^2}{2 k_B T}}. \tag{99}$$

Similarly, we can show that the expression determining the spatial average of static pressure p in the Knudsen layer is equal to

$$\bar{p}(y_{Kn}, w) = \int_{-\frac{L_0}{2}}^{\frac{L_0}{2}} p(x, y_{Kn}, w) \, dx$$
$$= p_0 e^{-\frac{m_p w^2}{2 k_B T}} \left(1 + \frac{m_p w^2}{3 k_B T}\right) + \frac{1}{3} \rho w^2 \left(e^{-\frac{m_p w^2}{2 k_B T}} - e^{-\frac{m_p w^2}{k_B T}}\right)$$
$$- \pi \sum_{m=1}^{\infty} \left[\frac{p_0}{12} a_m^2(w) + \frac{\rho w^2}{24} b_m^2(w)\right]. \tag{100}$$

In order to determine the spatial average of the shear stress component σ_{yx} in the Knudsen layer, given by Eq. (84), we can utilize the equality given by Eq. (89), which enables us to obtain the expression

$$\bar{\sigma}_{yx}(y_{Kn}, w) = \frac{1}{L_0} \int_{-\frac{L_0}{2}}^{\frac{L_0}{2}} \sigma_{yx}(x, y_{Kn}, w) \, dx$$
$$= -\frac{\pi^{\frac{3}{2}}}{16} \rho v_{th} w \sum_{m=1}^{\infty} a_m(w) b_m(w). \tag{101}$$

VII. RESULTS

All of the quantities in the Knudsen layer are determined for a flow of helium (He) gas near a monocrystalline copper surface—Cu (010). Temperature and pressure are taken to be $T = 298.15$ K and $p_0 = 1.01325$ bar. Mass of a single helium atom is equal to $m_p = 6.646\,476\,70 \times 10^{-27}$ kg,[58] while the two parameters h_0 and L_0 corresponding to peak-to-peak amplitude and wavelength for a potential pertaining to Cu (010) are both equal to $h_0 = 0.025 \times 10^{-10}$ m and $L_0 = 3.597 \times 10^{-10}$ m.[59]

Figures 5 and 6 display the statistical averages of fluid velocity components v_x and v_y as given by Eqs. (53) and (58), calculated for $w = 10$ m/s. They show us that the two velocity components have a $\cos x$ like dependence on the position x, meaning that they are both periodic functions. It is evident that v_x and v_y have the same
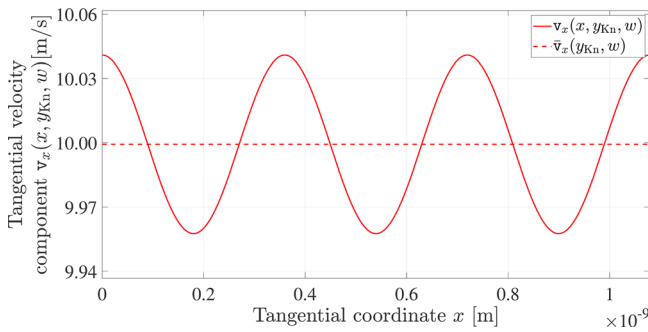
FIG. 5. Mesoscopic tangential velocity component v_x at $w = 10$ m/s.

FIG. 7. Spatial average of the tangential velocity component.

functional dependence as potential shape function f_S given by Eq. (4), as both components of fluid velocity match the contour which defines the shape of the potential. We can also note the fact that we can decompose both of the statistical averages into a constant term independent of x, which represents the spatial average of a velocity component, and an oscillatory term, which is a function of $\cos x$.

We can also observe that the spatial average of the normal velocity component v_y is equal to zero, which means there is no net flow of fluid in the direction of the y axis, while the spatial average of the tangential velocity component v_x is equal to a constant value, which is a function of the wall velocity w.

Figure 7 displays the spatial average of the tangential fluid velocity component v_x as a function of w as given by Eq. (92). We can observe that the spatial average changes linearly at a rate approximately equal to one, that is, $\bar{v}_x(w) \approx w$. This fact serves to demonstrate that when either the surface or fluid moves with a relatively small velocity w, the no-slip boundary condition represents a very good approximation of the relation between the surface and wall velocities. It should be noted that according to our model, tangential velocity $\bar{v}_x$ is strictly smaller than w for all $w > 0$, which makes sense because any momentum impaired by the moving surface upon the fluid is also dissipated in directions perpendicular to the direction of motion. This can also be deduced from the probability density function given by Eq. (42), which is more spread out on the interval of possible scattering angles θ at higher values of w, meaning that there is greater likelihood of particles scattering into directions, which deviate
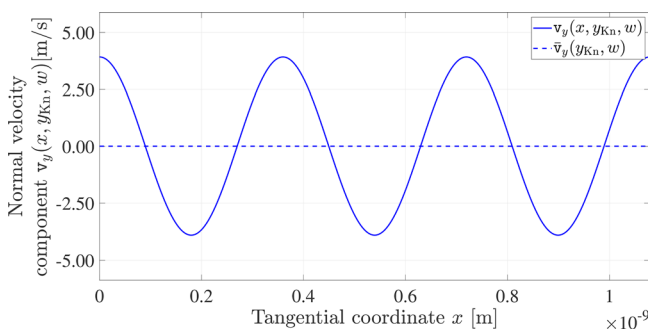
from the specular angle $\theta = -\theta'$. Furthermore, this property may also explain why tangential velocity reaches a maximum value with increasing w and behaves as e^{-kw^2} for values of w approaching infinity, where it approaches zero. Because we assumed that we are dealing with a sub-sonic flow where fluid density is constant everywhere in the domain, it is difficult to treat results at large values of w as entirely factual.

The amplitudes of the oscillating parts of v_x and v_y that can be extracted from Eqs. (53) and (58) are shown in Fig. 8. By comparing Figs. 7 and 8, we can observe that graphs of the amplitude of the oscillatory part of v_x and its spatial average have the same general shape in the sense of behaving as a linear functions for small values of wall velocity w, having a global maximum at some larger value of w and tapering off to zero for very large values of w. On the other hand, the amplitude of the oscillatory part of v_y is constant at small values of w and behaves as e^{-kw^2} at larger values.

We can observe from Figs. 9 and 10 that the diagonal stress tensor components and static pressure oscillate as a function of $\cos x$, while Figs. 11 and 12 show that the sole non-diagonal stress tensor component σ_{yx} is proportional to $\cos(kx) - a(w) \cos^2(kw)$, which is also evident from Eq. (84). Similarity between the oscillatory behaviors of stress tensor components and statistical averages of velocity components is a consequence of the fact that stresses in a fluid are a consequence of momentum fluxes in various directions, which depends on the velocities of constituent particles. This is a point conveyed by the expression (60).
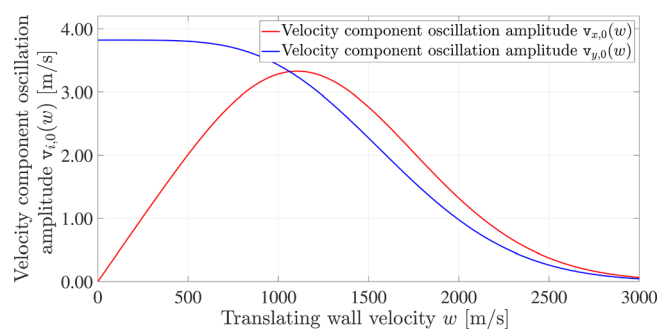

FIG. 6. Mesoscopic normal velocity component v_y at $w = 10$ m/s.

FIG. 8. Amplitudes of velocity component oscillations.
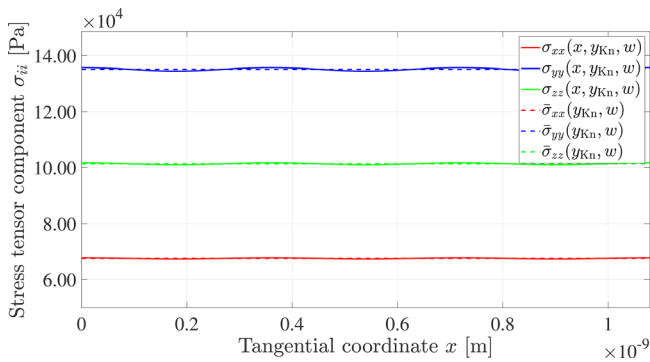
FIG. 9. Diagonal stress tensor components σ_{ii} at $w = 10$ m/s.
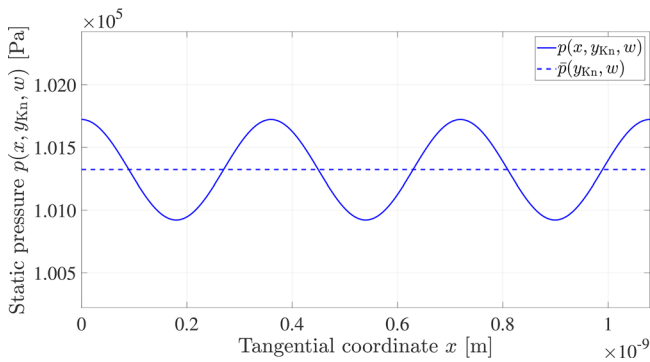
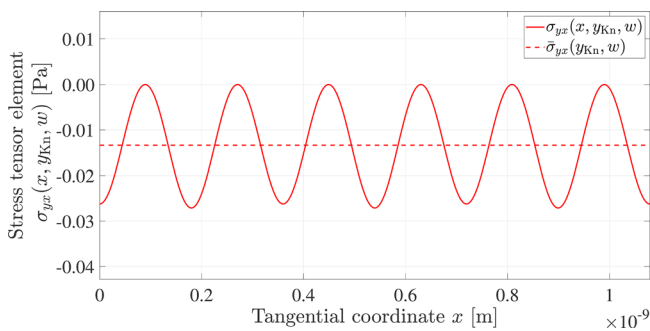**FIG. 10.** Static pressure p at $w = 10$ m/s.

FIG. 11. Stress tensor component σ_{yx} at $w = 10$ m/s.

FIG. 12. Stress tensor component σ_{yx} at $w = 100$ m/s.

FIG. 13. Spatial average of static pressure $\bar{p}$.
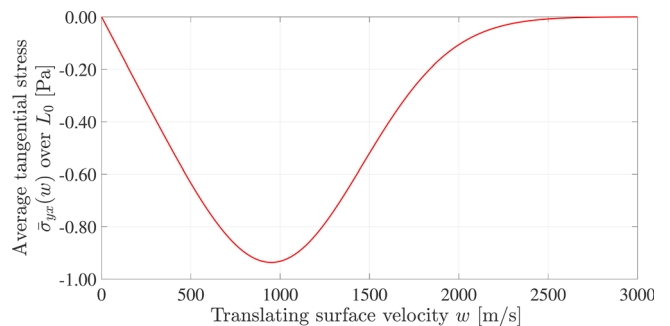
FIG. 14. Spatial average of tangential stress $\bar{\sigma}_{yx}$.

Figures 13 and 14 show how the spatial averages of the static pressure p and shear stress component σ_{yx} given by Eqs. (100) and (101) depend on wall velocity w. It is evident from the former figure that static pressure is constant at low values of w and then decreases proportionally to e^{-kw^2} as w increases. This is so because the e^{-kw^2} term in Eq. (100) dominates over the $w^2 e^{-kw^2}$ terms. The latter figure shows that the shear stress component σ_{yx} increases approximately
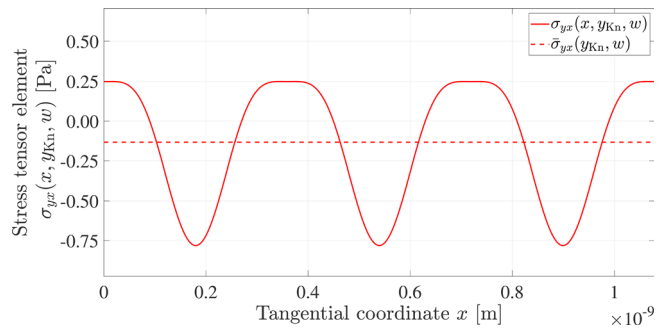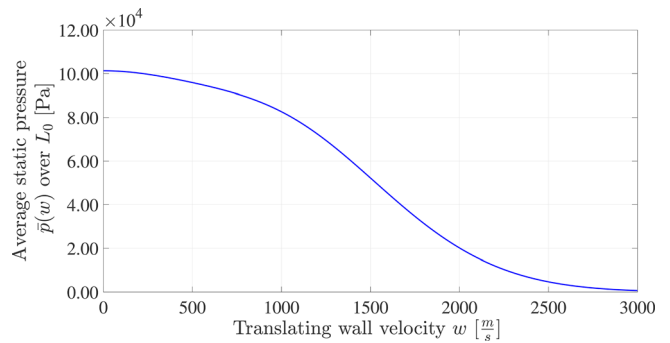
linearly for small values of w and then decreases proportionally to e^{-kw^2} after the shear stress reaches its maximum value with increasing w. Linear correlation between the wall velocity w and shear stress given by σ_{yx} also speaks in favor of the model, as this is an empirical law also observed in nature. It is well known that that the coefficient of drag c_d for a flat plate is inversely proportional to the velocity of the flow around the plate, which is why we can say that there exist definite similarities between the predictions of our model and empirical observations (at least at low values of the wall velocity w). It should be noted

here that because of certain approximations we have made in our model it is very difficult to predict values of the average shear stress in the Knudsen layer with a very high degree of accuracy. Therefore, it is also very difficult to compare our predictions directly with very precise empirical measurements of the drag coefficient for similar geometries.

VIII. DISCUSSION

In this paper, we have shown how the statistical averages, that is, mesoscopic velocity components v_x and v_y [Eqs. (53) and (58)] as well as stress tensor components and static pressure $\sigma_{xx}, \sigma_{yy}, \sigma_{zz}, \sigma_{yx,}$ and p, respectively, in the Knudsen layer [Eqs. (69), (75), (80), (84), and (81)] are periodic functions of the tangential coordinate x. Each of these functions can be expressed as a sum of parts, one of which is constant with respect to position and another that is a function of the tangential coordinate x and is represented by a Fourier series. We have also shown that the relationships between spatial averages of the tangential and normal velocity components $\bar{v}_x$ and $\bar{v}_y$ [Eqs. (91) and (92)], which are equal to average macroscopic values of these components, and wall velocity w match empirical observations relatively well. Our model predicts that the velocity component $\bar{v}_y$ is equal to zero for all values of w, while the velocity component $\bar{v}_x$ is equal to w for sufficiently small values of w, which is in accordance with the classical no-slip boundary condition based on empirical analysis of the flow of fluid near a surface. Furthermore, our model also predicts a linear relationship between fluid shear stress σ_{yx} in the Knudsen layer and velocity w in cases when its value is small, which is another result that matches empirically deduced trends, although discrepancies between exact values of shear predicted by our model and experimentally measured values are considerable. Interestingly, our model also predicts that the normal stress components in the Knudsen layer are not equal to each other as is usually the case in the bulk of the fluid, and that the spatial average of static pressure decreases with increasing wall velocity.

Another important fact evident from expressions for previously mentioned quantities in the Knudsen layer is the dependence of these quantities on the surface corrugation peak-to-peak amplitude h_0. Examining functions from Eqs. (57) and (51), which appear in expressions for v_x and v_y, see Eqs. (53) and (58), respectively, we can see that they decrease in value as h_0 approaches zero, meaning that both velocity components would also decrease. In fact, if the surfaces were completely flat (disregarding adsorption of fluid particles onto the surface), $h_0 = 0$, both velocity components v_x and v_y would be equal to zero, because there would be no tangential momentum transfer between the wall and fluid atoms/molecules due to specular collisions. It is necessary to point that according to the previously presented formalism, when $h_0 = 0$ is true, velocity v_x equals

$$v_x(h_0 \to 0) = w e^{-\frac{m_p w^2}{2 k_B T}}, \tag{102}$$

which would suggest that there would still exist some sort of momentum transfer between the surface and the fluid. However, we need to make a note that if the surface was ideally flat ($h_0 = 0$), particles' velocity component v_x would not change during collisions and scattering would be completely specular. Furthermore, from the viewpoint of fluid particles, an ideally flat moving surface with such properties is in fact completely indistinguishable from a stationary surface, while our whole formalism is based around the surface being in motion relative to the bulk of fluid. Therefore, our formalism breaks down when the corrugation amplitude h_0 is exactly zero, and expression (102)

represents a false limit case. In addition, as h_0 approaches zero, oscillations of static pressure p and shear stress component σ_{yx} decrease and approach zero as well, as does the spatial average of the shear stress.

We can summarize our previous findings by stating that if the surface of a moving wall is ideally flat, $h_0 = 0$, surface would slip past the body of fluid without any resistance, as is it would be unable to generate tangential stresses in the Knudsen layer (the same argument also applies to cases when fluid flows past a stationary flat surface). Our model might therefore explain the reason why friction occurs even when fluid flows past a hydraulically smooth surface, meaning that it has a certain roughness of the order of a length scale, which is smaller than the thickness of the viscous sub-layer. Skin friction in the case of turbulent flows at very high Reynolds numbers Re (Re $\to \infty$) is independent of the Reynolds number, but exhibits dependence on the relative roughness $\frac{\varepsilon}{L_0}$, with the skin friction coefficient of a hydraulically smooth surface having a value greater than zero. Considering that the surface of a monocrystalline body represents the best possible physical approximation of a hydraulically smooth surface, it might not be an exaggeration to state that the non-zero value of the coefficient of drag is a consequence of atomic length scale surface corrugation.

The obtained results are also interesting from the viewpoint of explaining boundary layer formation and hydrodynamic instability analysis. The prerequisite for the existence of a velocity boundary layer is the presence of tangential stresses in the solid–fluid interface, which itself can occur only if the solid has some sort of surface roughness present on the atomic length scale or some other larger scales. Additionally, even though velocity and stress oscillations predicted by our model occur on a mesoscopic length scale, it is possible that the phenomenon described in this paper also results in velocity and stress oscillations on the macroscopic length scale. Establishing a clear relationship between these two sets of quantities remains an unresolved problem, although we have reasons to believe that there exist potential avenues toward establishing such a relationship. One possible method consists of determining spatial averages of mesoscopic quantities on intervals which are of the order of the mean free path and interpolating between these discrete values in order to obtain a spatially continuous function. This function would represent a macroscopic quantity and therefore a boundary condition which could be utilized when solving, for example, Navier–Stokes equations, and would allow us to analyze the influence of velocity and stress oscillations on fluid flow as well as boundary layer formation and stability.

AUTHOR DECLARATIONS

Conflict of Interest

The authors have no conflicts to disclose.

DATA AVAILABILITY

The data that support the findings of this study are available from the corresponding author upon reasonable request.

APPENDIX: USEFUL MATHEMATICAL FORMULAS

$$(\cos\theta' + \cos\theta)^{2m} = \sum_{k=0}^{2m}\binom{2m}{k}\cos^k\theta\sum_{n=0}^{2m-k}\binom{2m-k}{n}\frac{e^{i(2(n-m)+k)\theta'}}{2^{2m-k}},$$

$$(A1)$$

$$\int_{-\frac{\pi}{2}}^{\frac{\pi}{2}} e^{i(2(n-m)+k)x}\,dx = \pi\,\mathrm{sinc}\left(\frac{\pi}{2}(2(n-m)+k)\right), \quad (A2)$$

$$\int_b^\infty x^n\,e^{-ax^2}\,dx = \frac{1}{2}\,a^{-\frac{n+1}{2}}\,\Gamma\left(\frac{n+1}{2},ab^2\right); \quad n\in\mathbb{Z}, \quad (A3)$$

$$\int_{-\frac{\pi}{2}}^{\frac{\pi}{2}} \sin(nx)\,\cos^k x\,dx = 0; \quad \Re(k)\ge 0,\ n\in\mathbb{Z}, \quad (A4)$$

$$\int_{-\frac{\pi}{2}}^{\frac{\pi}{2}} \cos^k x\,dx = \sqrt{\pi}\,\frac{\Gamma\left(\frac{k+1}{2}\right)}{\Gamma\left(\frac{k+2}{2}\right)}; \quad \Re(k)\ge 0,\ k\in\mathbb{Z}, \quad (A5)$$

$$\int_{-\frac{\pi}{2}}^{\frac{\pi}{2}} \sin^2 x\,\cos^k x\,dx = \frac{\sqrt{\pi}}{2}\,\frac{\Gamma\left(\frac{k+1}{2}\right)}{\Gamma\left(\frac{k+4}{2}\right)}; \quad \Re(k)\ge 0,\ k\in\mathbb{Z}, \quad (A6)$$

$$\overline{f(w)g(w)} = \frac{1}{L_0}\int_{-\frac{L_0}{2}}^{\frac{L_0}{2}} f(x,w)g(x,w)\,dx$$

$$= \frac{1}{L_0}\int_{-\frac{L_0}{2}}^{\frac{L_0}{2}} \sum_{m=1}^\infty f_m(w)\cos\left(\frac{2\pi m}{L_0}x\right)\sum_{m=1}^\infty g_m(w)\cos\left(\frac{2\pi m}{L_0}x\right)dx$$

$$= \frac{1}{L_0}\int_{-\frac{L_0}{2}}^{\frac{L_0}{2}} \left(\sum_{m=1}^\infty f_m(w)g_m(w)\cos^2\left(\frac{2\pi m}{L_0}x\right)\right.$$

$$+ \frac{1}{2}\sum_{\substack{m=1\\m\neq n}}^\infty\sum_{n=1}^\infty f_m(w)g_n(w)\left(\cos\left(\frac{2\pi(m+n)}{L_0}x\right)\right.$$

$$\left.\left. + \cos\left(\frac{2\pi(m-n)}{L_0}x\right)\right)\right)dx$$

$$= \frac{1}{L_0}\sum_{m=1}^\infty f_m(w)g_m(w)\int_{-\frac{L_0}{2}}^{\frac{L_0}{2}}\cos^2\left(\frac{2\pi m}{L_0}x\right)dx$$

$$= \frac{1}{2}\sum_{m=1}^\infty f_m(w)g_m(w). \quad (A7)$$

NOMENCLATURE

c	Auxiliary function in the expression for the function P_G, /
c_i	Component of relative velocity, m/s
c_1	Auxiliary constant in the expression for the function P, s/m
c_2	Auxiliary constant in the expression for the Maxwell–Boltzmann probability density function, s/m
d	Particle kinetic diameter, m
$\mathscr{F}_0$	Auxiliary function of coordinate x No. 0, /
$\mathscr{F}_1$	Auxiliary function of coordinate x No. 1, /
$\mathscr{F}_2$	Auxiliary function of coordinate x No. 2, /
$\mathscr{F}_3$	Auxiliary function of coordinate x No. 3, /
$\mathscr{F}_4$	Auxiliary function of coordinate x No. 4, /
f	Velocity probability density function, s^3/m^3
f_{inc}	Probability density function of a particle entering the Knudsen layer, /
f_S	Potential shape function, /
f_0	Maxwell–Boltzmann distribution, s^3/m^3
f^-	Velocity probability density function of incident particles, s^3/m^3
f^+	Velocity probability density function of scattered particles, s^3/m^3
h	Planck's constant, m^2 kg/s
h_0	Peak-to-peak corrugation amplitude, m
k	Particle wave vector, 1/m
k_B	Boltzmann constant, J/K
L_{Kn}	Knudsen layer thickness, m
L_0	Corrugation wavelength, m
l_{mfp}	Molecular mean free path, m
m_p	Particle mass, kg
n	Number density, 1/m^3
P	Full conditional probability density function, s/m
P_G	Summation coefficient in the expansion of function P_θ, /
P_θ	Angular probability density of scattering function, /
p	Pressure, Pa
p_0	Thermodynamically defined pressure, Pa
T	Temperature, K
t	Time, s
u_i	Velocity component in the local reference frame, m/s
u_z	Perpendicular direction velocity magnitude in the local reference frame, m/s
u_0	Azimuthal plane velocity magnitude in the local reference frame, m/s
v_i	Mesoscopic velocity component, m/s
v_i	Velocity component in the global reference frame, m/s
v_{th}	Thermal velocity, m/s
v_z	Perpendicular direction velocity magnitude in the global reference frame, m/s
v_0	Azimuthal plane velocity magnitude in the global reference frame, m/s
w	Translating wall velocity, m/s
x	Tangential position coordinate in the local reference frame, m
y	Normal position coordinate in the local reference frame, m
z	Perpendicular position coordinate in the local reference frame, m
Θ	Azimuthal angle of the velocity vector in the global reference frame, /
θ	Azimuthal angle of the velocity vector in the local reference frame, /
κ	Auxiliary constant in the expression for the function P_θ, /
λ_{DB}	De Broglie wavelength, m
ρ	Fluid density, kg/m^3
σ_{ij}	Stress tensor component, Pa
ψ	General quantity, /

REFERENCES

[1] M. Kadivar, D. Tormey, and G. McGranaghan, "A review on turbulent flow over rough surfaces: Fundamentals and theories," Int. J. Thermofluids **10**, 100077 (2021).

[2]V. Dharaiya and S. Kandlikar, "A numerical study on the effects of 2d structured sinusoidal elements on fluid flow and heat transfer at microscale," Int. J. Heat Mass Transfer **57**, 190–201 (2013).

[3]A. Rouhi, D. Chung, and N. Hutchins, "Direct numerical simulation of open-channel flow over smooth-to-rough and rough-to-smooth step changes," J. Fluid Mech. **866**, 450–486 (2019).

[4]C. Cercignani, *Mathematical Methods in Kinetic Theory* (Springer, 1969).

[5]F. Sharipov and V. Seleznev, "Data on internal rarefied gas flows," J. Phys. Chem. Ref. Data **27**, 657–706 (1998).

[6]V. Roldughin and V. Zhdanov, "Non-equilibrium thermodynamics and kinetic theory of gas mixtures in the presence of interfaces," Adv. Colloid Interface Sci. **98**, 121–215 (2002).

[7]F. Golse, "Analysis of the boundary layer equation in the kinetic theory of gases," Bull. Inst. Math., Acad. Sin. (New Ser.) **3**, 211–242 (2008).

[8]S. Takata, "Symmetry of the linearized Boltzmann equation and its application," J. Stat. Phys. **136**, 751–784 (2009).

[9]C. Cercignani, "The Kramers problem for a not completely diffusing wall," J. Math. Anal. Appl. **10**, 568–586 (1965).

[10]C. Cercignani and S. Lorenzani, "Variational derivation of second-order slip coefficients on the basis of the Boltzmann equation for hard-sphere molecules," Phys. Fluids **22**, 062004 (2010).

[11]S. K. Loyalka, "Approximate method in the kinetic theory," Phys. Fluids **14**, 2291–2294 (1971).

[12]S. Loyalka, "The slip problems for a simple gas," Z. Naturforsch., A: Phys. Sci. **26**, 964–972 (1971).

[13]T. Klinc and I. Kuščer, "Slip coefficients for general gas-surface interaction," Phys. Fluids **15**, 1018–1022 (1972).

[14]C. Siewert, "Viscous-slip, thermal-slip, and temperature-jump coefficients as defined by the linearized Boltzmann equation and the Cercignani–Lampis boundary condition," Phys. Fluids **15**, 1696–1701 (2003).

[15]R. Garcia and C. Siewert, "The linearized Boltzmann equation with Cercignani–Lampis boundary conditions: Basic flow problems in a plane channel," Eur. J. Mech.-B/Fluids **28**, 387–396 (2009).

[16]R. Garcia and C. Siewert, "Viscous-slip, thermal-slip, and temperature-jump coefficients based on the linearized Boltzmann equation (and five kinetic models) with the Cercignani–Lampis boundary condition," Eur. J. Mech.-B/Fluids **29**, 181–191 (2010).

[17]L. Wu and H. Struchtrup, "Assessment and development of the gas kinetic boundary condition for the Boltzmann equation," J. Fluid Mech. **823**, 511–537 (2017).

[18]N. N. Nguyen, I. Graur, P. Perrier, and S. Lorenzani, "Variational derivation of thermal slip coefficients on the basis of the Boltzmann equation for hard-sphere molecules and Cercignani–Lampis boundary conditions: Comparison with experimental results," Phys. Fluids **32**, 102011 (2020).

[19]H. Chen, "Cercignani–Lampis boundary in the Boltzmann theory," arXiv:1906.01808 (2019).

[20]S. Wang, A. A. Lukyanov, L. Wang, Y.-S. Wu, A. Pomerantz, W. Xu, and R. Kleinberg, "A non-empirical gas slippage model for low to moderate Knudsen numbers," Phys. Fluids **29**, 012004 (2017).

[21]S. Wang, A. A. Lukyanov, and Y.-S. Wu, "Second-order gas slippage model for the Klinkenberg effect of multicomponent gas at finite Knudsen numbers up to 1," Fuel **235**, 1275–1286 (2019).

[22]H. Nakano and S.-i. Sasa, "Statistical mechanical expressions of slip length," J. Stat. Phys. **176**, 312–357 (2019).

[23]J. De La Torre, D. Duque-Zumajo, D. Camargo, and P. Español, "Microscopic slip boundary conditions in unsteady fluid flows," Phys. Rev. Lett. **123**, 264501 (2019).

[24]E. Gross, E. Jackson, and S. Ziering, "Boundary value problems in kinetic theory of gases," Ann. Phys. **1**, 141–167 (1957).

[25]E. Gross and S. Ziering, "Kinetic theory of linear shear flow," Phys. Fluids **1**, 215–224 (1958).

[26]S. Ziering, "Flow of a gas near a solid surface," AIAA J. **1**, 661–664 (1963).

[27]K. Aoki, Y.-C. Lin, and K.-C. Wu, "Milne problem for the linear and linearized Boltzmann equations relevant to a binary gas mixture," J. Differ. Equations **269**, 257–287 (2020).

[28]S. Brull, P. Charrier, and L. Mieussens, "Gas-surface interaction and boundary conditions for the Boltzmann equation," arXiv:1306.4309 (2013).

[29]F. Coron, "Derivation of slip boundary conditions for the Navier–Stokes system from the Boltzmann equation," J. Stat. Phys. **54**, 829–857 (1989).

[30]S. Shen, G. Chen, R. M. Crone, and M. Anaya-Dufresne, "A kinetic-theory based first order slip boundary condition for gas flow," Phys. Fluids **19**, 086101 (2007).

[31]M. Hattori, S. Kosuge, and K. Aoki, "Slip boundary conditions for the compressible Navier–Stokes equations for a polyatomic gas," Phys. Rev. Fluids **3**, 063401 (2018).

[32]K. Aoki, C. Baranger, M. Hattori, S. Kosuge, G. Martalo, J. Mathiaud, and L. Mieussens, "Slip boundary conditions for the compressible Navier–Stokes equations," J. Stat. Phys. **169**, 744–781 (2017).

[33]S. Kosuge, K. Aoki, M. Bisi, M. Groppi, and G. Martalò, "Boundary conditions for two-temperature Navier–Stokes equations for a polyatomic gas," Phys. Rev. Fluids **6**, 083401 (2021).

[34]R. Duan and S. Liu, "Compressible Navier–Stokes approximation for the Boltzmann equation in bounded domains," Trans. Am. Math. Soc. **374**, 7867–7924 (2021).

[35]Y. Ben-Ami and A. Manela, "The effect of a solid boundary on the propagation of thermodynamic disturbances in a rarefied gas," Phys. Fluids **32**, 092002 (2020).

[36]G. Silva and V. Semiao, "Consistent lattice Boltzmann modeling of low-speed isothermal flows at finite Knudsen numbers in slip-flow regime: Application to plane boundaries," Phys. Rev. E **96**, 013311 (2017).

[37]G. Silva and I. Ginzburg, "Reviving the local second-order boundary approach within the two-relaxation-time lattice Boltzmann modelling," Philos. Trans. R. Soc., A **378**, 20190404 (2020).

[38]S. Mohammed and T. Reis, "Lattice Boltzmann method with moment-based boundary conditions for rarefied flow in the slip regime," Phys. Rev. E **104**, 045309 (2021).

[39]B. Shan, P. Wang, Y. Zhang, and Z. Guo, "Discrete unified gas kinetic scheme for all Knudsen number flows. IV. Strongly inhomogeneous fluids," Phys. Rev. E **101**, 043303 (2020).

[40]J. Ou and J. Chen, "Nonlinear transport of rarefied Couette flows from low speed to high speed," Phys. Fluids **32**, 112021 (2020).

[41]T. Liang, J. Zhang, and Q. Li, "A parameter-free physical model for gas–surface interaction," Phys. Fluids **33**, 082005 (2021).

[42]S. Varghese, J. Hansen, and B. Todd, "Improved methodology to compute the intrinsic friction coefficient at solid–liquid interfaces," J. Chem. Phys. **154**, 184707 (2021).

[43]O. E. Lanford, "Time evolution of large classical systems," in *Dynamical Systems, Theory and Applications* (Springer, 1975), pp. 1–111.

[44]R. Illner and M. Pulvirenti, "Global validity of the Boltzmann equation for a two-dimensional rare gas in vacuum," Commun. Math. Phys. **105**, 189–203 (1986).

[45]Y. E. Kuzovlev, "Bbgky equations, self-diffusion and 1/f noise in a slightly non-ideal gas," arXiv:0907.3475 (2009).

[46]R. Esposito, Y. Guo, and R. Marra, "Validity of the Boltzmann equation with an external force," Kinet. Relat. Models **4**, 499 (2011).

[47]I. Gallagher, "From newton to Navier–Stokes, or how to connect fluid mechanics equations from microscopic to macroscopic scales," Bull. Am. Math. Soc. **56**, 65–85 (2019).

[48]F. O. Goodman, *Dynamics of Gas-Surface Scattering* (Elsevier, 2012).

[49]K. W. Ford and J. A. Wheeler, "Semiclassical description of scattering," Ann. Phys. **7**, 259–286 (1959).

[50]R. I. Masel, R. P. Merrill, and W. H. Miller, "Quantum scattering from a sinusoidal hard wall: Atomic diffraction from solid surfaces," Phys. Rev. B **12**, 5545 (1975).

[51]J. Manson, H. Khemliche, and P. Roncin, "Theory of grazing incidence diffraction of fast atoms and molecules from surfaces," Phys. Rev. B **78**, 155408 (2008).

[52]F. O. Goodman, "Scattering of atoms by a stationary sinusoidal hard wall: Rigorous treatment in $(n+1)$ dimensions and comparison with the Rayleigh method," J. Chem. Phys. **66**, 976–982 (1977).

[53]U. Garibaldi, A. Levi, R. Spadacini, and G. Tommei, "Quantum theory of atom-surface scattering: Diffraction and rainbow," Surf. Sci. **48**, 649–675 (1975).

[54]D. Farias and K.-H. Rieder, "Atomic beam diffraction from solid surfaces," Rep. Prog. Phys. **61**, 1575 (1998).

[55]B. Gumhalter, "Single- and multiphonon atom–surface scattering in the quantum regime," Phys. Rep. **351**, 1–159 (2001).

[56]R. Guantes, A. Sanz, J. Margalef-Roig, and S. Miret-Artés, "Atom–surface diffraction: A trajectory description," Surf. Sci. Rep. **53**, 199–330 (2004).

[57]J. Manson, "Theoretical aspects of atom-surface scattering," in *Helium Atom Scattering from Surfaces* (Springer, 1992), pp. 173–205.

[58]N. B. Vargaftik, *Handbook of Physical Properties of Liquids and Gases-Pure Substances and Mixtures* (Springer Berlin Heidelberg, 1975).

[59]W. P. Davey, "Precision measurements of the lattice constants of twelve common metals," Phys. Rev. **25**, 753 (1925).